Hard Superconducting Gap in PbTe Nanowires

Yichun Gao(高益淳)[1†], Wenyu Song(宋文玉)[1†], Shuai Yang(杨帅)[1†], Zehao Yu(于泽昊)[1], Ruidong Li(李睿东)[1], Wentao Miao(苗文韬)[1], Yuhao Wang(王禹灏)[1], Fangting Chen(陈芳婷)[1], Zuhan Geng(耿祖汗)[1], Lining Yang(杨利宁)[1], Zezhou Xia(夏泽洲)[1], Xiao Feng(冯硝)[1,2,3,4], Yunyi Zang(臧运祎)[2,4], Lin Li(李琳)[2], Runan Shang(尚汝南)[2,4], Qi-Kun Xue(薛其坤)[1,2,3,4,5], Ke He(何珂)[1,2,3,4*], and Hao Zhang(张浩)[1,2,3*]

[1]*State Key Laboratory of Low Dimensional Quantum Physics, Department of Physics, Tsinghua University, Beijing 100084, China*
[2]*Beijing Academy of Quantum Information Sciences, Beijing 100193, China*
[3]*Frontier Science Center for Quantum Information, Beijing 100084, China*
[4]*Hefei National Laboratory, Hefei 230088, China*
[5]*Southern University of Science and Technology, Shenzhen 518055, China*

(Received 22 December 2023; accepted manuscript online 26 February 2024)

Semiconductor nanowires coupled to a superconductor provide a powerful testbed for quantum device physics such as Majorana zero modes and gate-tunable hybrid qubits. The performance of these quantum devices heavily relies on the quality of the induced superconducting gap. A hard gap, evident as vanishing subgap conductance in tunneling spectroscopy, is both necessary and desired. A hard gap has been achieved and extensively studied before in Ⅲ–V semiconductor nanowires (InAs and InSb). In this study, we present the observation of a hard superconducting gap in PbTe nanowires coupled to a superconductor Pb. The gap size Δ is $\sim$1 meV (maximally 1.3 meV in one device). Additionally, subgap Andreev bound states can also be created and controlled through gate tuning. Tuning a device into the open regime can reveal Andreev enhancement of the subgap conductance. These results pave the way for diverse superconducting quantum devices based on PbTe nanowires.

DOI: 10.1088/0256-307X/41/3/038502

A superconductor can induce superconductivity in a semiconductor through proximity coupling. This coupling was spatially non-uniform in early devices due to disorder at the semiconductor-superconductor interface.[1] While supercurrent can still be clearly resolved in Josephson devices,[2] the induced superconducting gap was soft with many quasi-particle states inside the gap. The soft gap can significantly degrade the quality of the corresponding device,[3] through mechanisms such as dissipation smearing or quasi-particle poisoning. Semiconductor nanowires provide a natural platform to study the induced superconducting gap, where an electrostatic gate can readily define a point contact for tunneling spectroscopy. The tunneling conductance reflects the density of states and can thus be associated with the quality of the induced superconducting gap. The issue of a soft gap in semiconductor nanowires can be addressed by suppressing interface disorder.[4,5] Furthermore, epitaxial growth of superconductors can yield atomically sharp interfaces and hard gaps.[6–9] These material improvements enable high quality quantum devices, e.g., on Majorana experiments[10–18] and hybrid qubits.[19–24] So far, most of the hard gap studies are based on Ⅲ–V semiconductors such as InAs or InSb. The Majorana theory[25,26] requires a clean semiconductor nanowire while the current experiments are disorder-limited.[27–31]

PbTe nanowires have been recently proposed[32] to overcome the disorder issue, owing to their large dielectric constant ($\sim$1350). Meanwhile, these nanowires have been grown using selective area epitaxy[33,34] and subjected to quantum transport characterization.[35–37] The superconducting proximity effect has also been demonstrated in PbTe-Pb Josephson junctions.[38] While a superconducting gap with a size of $\Delta \sim 0.4$ meV can be inferred, it is essential to note that tunneling spectroscopy in a Josephson device does not directly unveil the quasiparticle density of states (DOS) but rather a convolution of them. Moreover, the subgap conductance may have other contributions from the supercurrent and multiple Andreev reflections. Therefore, to directly probe the induced gap, N-NW-S devices are needed (where N stands for normal metal, NW for nanowire and S for superconductor). We have recently improved the material quality and here demonstrate the hard superconducting gap in PbTe nanowires in N-NW-S devices. We used Pb as the superconductor and measured a superconducting gap of $\Delta \sim 1$ meV. This value is comparable to those observed in InAs-Pb devices[39] and significantly larger than those

†These authors contributed equally to this work.
*Corresponding authors. Email: kehe@tsinghua.edu.cn; hzquantum@mail.tsinghua.edu.cn
© 2024 Chinese Physical Society and IOP Publishing Ltd

reported in our early devices.[38] Andreev bound states (ABSs) can be generated and controlled by gate voltages, providing an additional material platform for investigating Andreev physics. These results are a pivotal advancement in utilizing PbTe nanowires for advanced quantum devices.

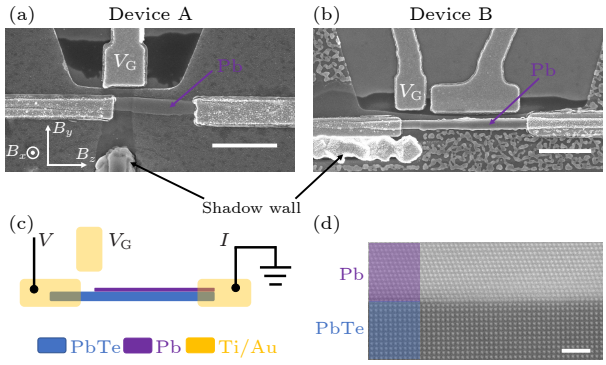

Fig. 1. Device basics. [(a), (b)] SEMs of devices A and B, respectively. Scale bar: 1 µm. The right gate in device B was kept grounded during the measurement. (c) Schematic of the device and measurement circuit: PbTe nanowire (blue), Pb superconductor (purple), contacts and gate (yellow). (d) STEM of a typical PbTe-Pb interface grown under identical conditions. Scale bar: 2 nm.

Figures 1(a) and 1(b) depict scanning electron micrographs (SEMs) of two devices (A and B). The PbTe nanowires were grown on a CdTe(001)/$Pb_{1-x}Eu_xTe$ substrate, and subsequently covered epitaxially with a thin Pb film (thickness ∼10 nm) and a CdTe capping layer. The value of x is estimated to be 0.01. The substrate was cooled using liquid nitrogen during the Pb growth process. The Pb film on the substrate of device B is discontinuous, likely due to the relatively high temperature during that particular growth. Nonetheless, the Pb films on the PbTe nanowires in both devices are uniform and continuous. The barrier region of the nanowire is defined by pre-patterned Hydrogen SilsesQuioxane (HSQ) shadow wall. The barrier transmission can be tuned by applying a voltage (V_G) to the side gate. The source and drain contacts, along with the side gates, were fabricated using evaporated Ti/Au (7/60 nm). Details of device fabrication can be found in the Supplemental Material. Standard two-terminal measurement was performed in a dilution fridge at its base temperature (below 50 mK). Figure 1(c) shows a simplified circuit and the schematic of the N-NW-S device. The scanning transmission electron microscopy (STEM) image in Fig. 1(d) displays a PbTe-Pb interface that was grown under identical conditions. An atomically sharp interface is crucial for the observation of a hard induced gap.

Figure 2(a) illustrates the conductance spectroscopy of device A over a large bias (V) range. The magnetic field (B) was kept at zero. The differential conductance, $G \equiv dI/dV$, was acquired using the standard lock-in technique. Note that the line resistance, mainly contributed by the fridge filters, has been subtracted from G. Additionally, V has also been corrected by subtracting the bias drop over the line resistance. The two horizontal lines near $V = \pm 1$ mV are the coherence peaks that feature the edges of the superconducting gap. To better resolve the gap, Fig. 2(b) shows a fine scan over a smaller V range. More negative V_G depletes the barrier region and pinches off the device. Near the pinch-off regime, the tunneling conductance is proportional to the DOS of the proximitized PbTe. The line cut [Fig. 2(c)] shows sharp coherence peaks and vanishing sub-gap conductance, indicating a hard superconducting gap. The suppression of conductance (outside-gap vs sub-gap) can reach two orders of magnitude, see Fig. S1 in the Supplemental Material for the log-scale plot. The bias values of the coherence peaks suggest a gap size $\Delta \sim 1$ meV, significantly larger than that of Al (∼0.2–0.3 meV). A large superconducting gap is favorable for Majorana research as it sets an upper limit for the size of the topological gap. Larger gap can "tolerate" stronger disorder. Compared to the previous work on InAs-Pb nanowires,[39] the gap size is similar but the coherence peaks here seem more sharply defined. Sharper coherence peaks suggest less dissipation smearing arising from undesirable quasi-particles.[40]

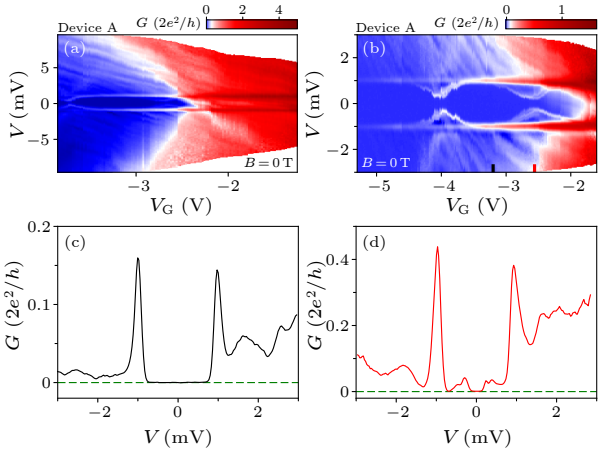

Fig. 2. Hard gap in device A. (a) G vs V and V_G at zero field over a large V range. (b) A fine scan over a smaller V range. (c) A line cut from (b) at $V_G = -3.24$ V, see the black bar in (b). (d) A line cut of the subgap states at $V_G = -2.56$ V, see the red bar in (b).

Besides the hard gap, another notable feature is the discrete sub-gap levels at particular gate voltages. These gate-tunable levels are ABSs, revealed as sub-gap conductance peaks [see Fig. 2(d) for a line cut]. ABSs are widely present in hybrid devices[41–45] and can mimic Majorana signatures, causing the decade-long debate.[46–52] ABSs usually originate in quantum dots coupled to superconductors. Figures 2(a) and 2(b) show no obvious Coulomb blockades except for single resonant levels near $V_G = -4$ V and $V_G = -2.5$ V. The white boundaries demarcating the red and blue regions in the color map suggest diamond-like shapes, see the dashed lines in Fig. S1(a). These diamonds are unlikely to be Coulomb blockades, considering that the charging energy in PbTe should be two orders of magnitude smaller.[36] The diamond slopes likely correspond to the subband bottoms of a quantum point contact.[37] In

Fig. S1 we show possible indication of quasi-ballistic transport of Fig. 2(a). In the absence of quantum dots, the observed ABSs are likely formed due to the smooth potential variation.[46,47]

The overall conductance is asymmetric for positive and negative biases. For example, the conductance in the positive bias branch is larger compared to that in the negative bias case. This trend may be due to the crosstalk between the bias and gate voltage. The large dielectric constant of PbTe greatly enhances the capacitive coupling and the charge tunability in the barrier region by the bias voltage. Similar trend has also been observed before in our PbTe nanowire devices.[37,53]

The outside-gap conductance exhibits Fabry–Pérot-like oscillations over V_{G}, possibly caused by the scattering between the barrier region and the drain contact. These oscillations can also affect the estimation of the normal state conductance (G_{N}). In Fig. S1, we present the extracted G_{N} plotted against G_{S}, i.e., $G(V = 0)$. We also compare it with the BTK-Beenakker formula[54,55] for illustrative purposes. Deviation between the formula and experiment exists and may arise from various factors. Firstly, the aforementioned oscillations make the estimation of G_{N} inaccurate. Secondly, the gap size of 1 meV is a significant fraction of the subband spacing in PbTe.[37] Unlike the scenario of Al with a much smaller gap, the outside-gap (large-bias) conductance in PbTe-Pb may not accurately reflect the barrier transmission (normal state conductance) at zero bias. Lastly, a crucial factor is that the BTK-Beenakker formula assumes a single channel in the barrier, which may not always hold. Moreover, even for the single channel case, the formula only holds for high chemical potentials,[56] thus has limited implications.

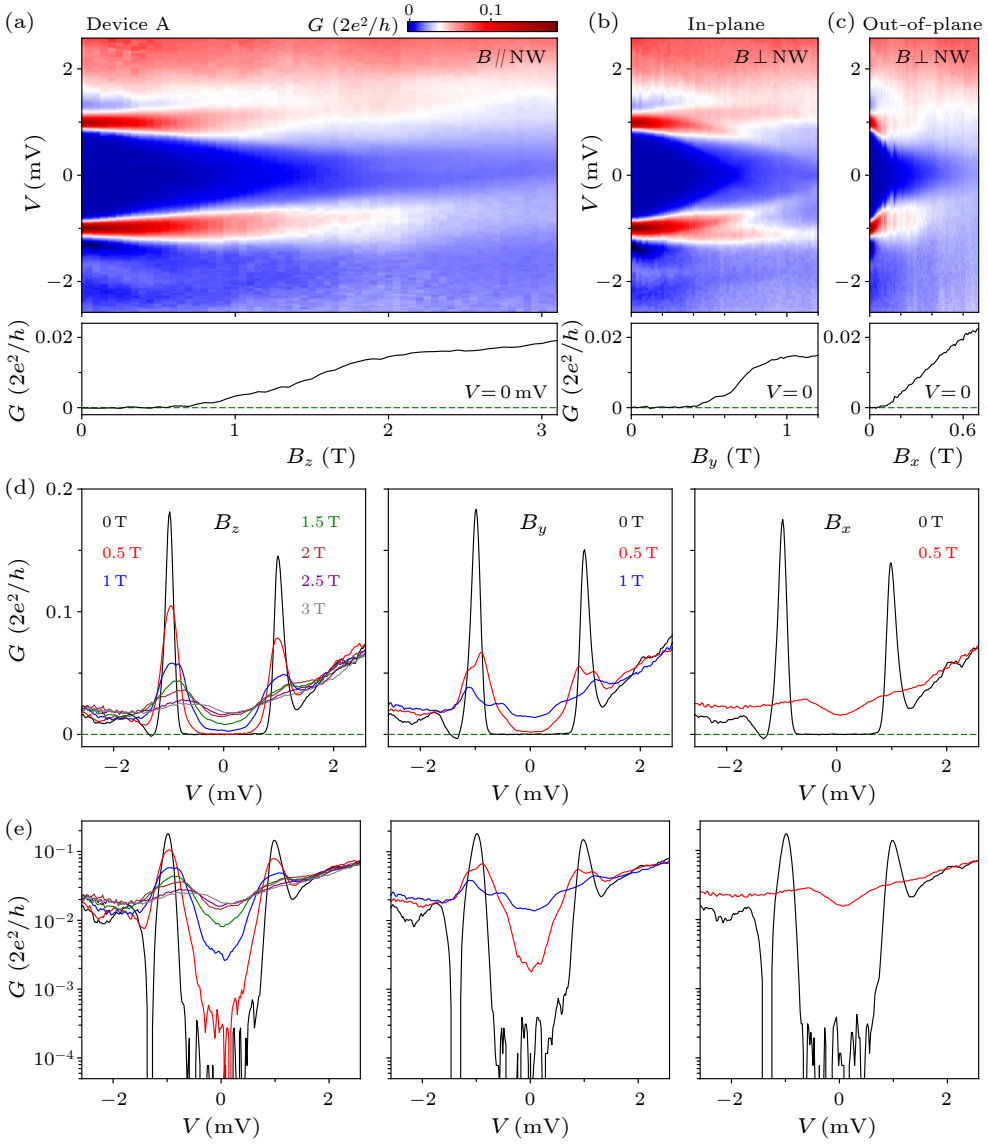

Fig. 3. B dependence of the hard gap. (a) G vs V and B_z (parallel to the nanowire). Lower panel, zero-bias line cut. [(b), (c)] B_y (in-plane) and B_x (out-of-plane) scans of the gap. Both are perpendicular to the nanowire. (d) Line cuts at different B's from (a)–(c). (e) Log-scale plot of (d). $V_{\mathrm{G}} = -2.7$ V for all panels.

We next study the B dependence of the hard gap (for the B dependence of ABSs, see Fig. S2 in the Supplemental Material). Figures 3(a)–3(c) show the B scans along three coordinate axes, see Fig. 1(a) for the labeling. B_z is roughly parallel to the nanowire (with an accuracy within 10°). The gap becomes soft for B_z approaching 1 T, see the lower panel for the zero-bias line cut. The gap closes as B_z approaches 2 T. The other two directions, B_y (in-plane) and B_x (out-of-plane), are both perpendicular to the nanowire. In the B_y scan, the gap closes at a lower field ($\sim$1 T) than the B_z case; while in the B_x scan, an even lower field ($\sim$0.5 T) is sufficient to close the gap. We attribute the gap closing in the B_x scan to the orbital effect, given that B_x is perpendicular to the Pb film. As for B_z and B_y, the orbital effect is smaller, as both directions are in-plane (parallel to the Pb film). A possible explanation of the anisotropy between B_z and B_y could be spin–orbit interaction. B_z aligns with the nanowire, therefore is perpendicular to the spin-orbit direction ($B_{\rm SO}$). Spin-orbit interaction protects the gap from closing when B is perpendicular to $B_{\rm SO}$, thus a higher critical field is observed for B_z. B_y is parallel to $B_{\rm SO}$. Hence the gap closes without the protection and a lower critical field is observed. Spin-orbit-induced anisotropy has been demonstrated before in InSb nanowires coupled to a superconductor NbTiN.[57]

Figures 3(d) and 3(e) illustrate line cuts at different fields in linear and logarithmic scales for these three directions to further illustrate this anisotropy. At zero field, the gap shows a conductance suppression over two orders of magnitude. At 0.5 T (the red curves), the gap still remains hard in the B_z scan while the sub-gap conductance has already been increased by an order of magnitude in the B_y scan and by two orders of magnitude in the B_x scan. In Fig. S3 of the Supplemental Material, we present a similar B anisotropy observed in another device. Note that in the InAs-Pb work,[39] the hard gap can persist to a considerable high B ($\sim$8.5 T). Further increasing the critical field for PbTe nanowires should be achievable and can be a topic for our forthcoming optimization efforts.

Negative differential conductance (NDC) can be observed outside the gap in Figs. 3(d)–3(e) in the negative bias branch. The positive bias branch exhibits a dip feature, but does not cross zero, possibly due to the asymmetric trend mentioned above. The NDC disappears upon increasing B. In fact, NDC is also present in Figs. 2(a) and 2(b), see Fig. S4 for a different color setting highlighting the NDC. The NDC is also present inside the gap, following subgap states in Fig. 2 possibly due to the formation of unintentional quantum dots. In a quantum dot asymmetrically coupled to superconductors, NDC can arise.[58–61] In our case, the "dot" or discrete level is, however, poorly defined by the Fabry–Pérot-like scatterings, thus a systematic study of NDC is not applicable.

For reproducibility purpose, we present two additional devices (B and C) in Fig. 4 demonstrating hard gaps. One more device (device D) can also be found in Fig. S3. Figure 4(a) shows the conductance map of device B. In the tunneling regime, a gap of $\Delta \sim 1.05$ meV is observed, see Fig. 4(b) for a line cut. NDC is also present outside the gap, closely following the Fabry–Pérot oscillations (see Fig. S4 for its highlight). In the open regime where the outside-gap conductance is close to $2e^2/h$, the subgap conductance is enhanced relative to the outside-gap conductance, as shown in Fig. 4(c). This enhancement is due to Andreev reflection. The enhancement factor is $\sim$1.7. Using the BTK-Beenakker formula $G_{\rm S} = 1.7 \times 2e^2/h = \frac{2T^2}{(2-T)^2} \times 2e^2/h$,[54,55] we can estimate the PbTe-Pb interface transparency $T \sim 0.96$. Note that this value is a rough estimation due to the conductance asymmetry for negative and positive biases.

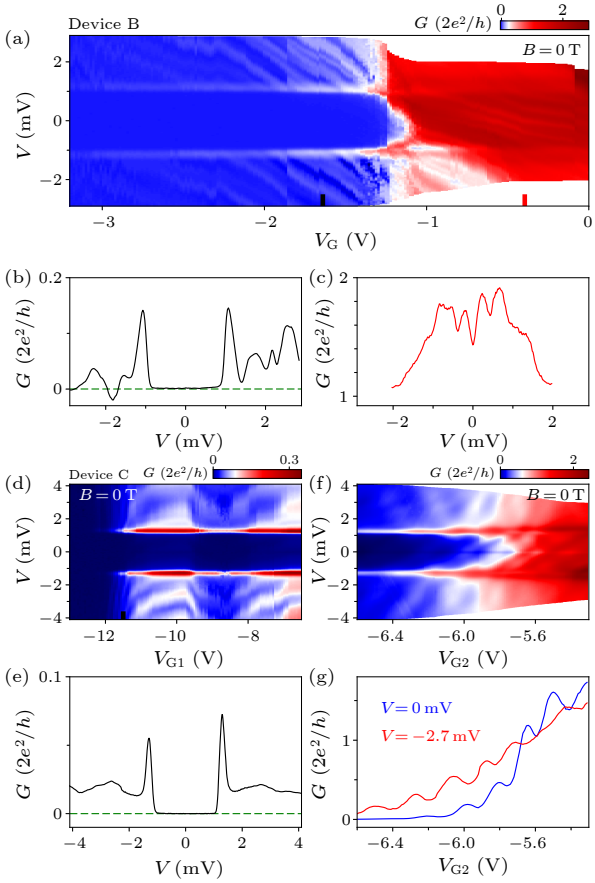

Fig. 4. Hard gap in devices B and C. (a) G vs V and $V_{\rm G}$ in device B at zero field. (b) A line cut from (a) at $V_{\rm G} = -1.64$ V (the tunneling regime). (c) A line cut from (a) at $V_{\rm G} = -0.395$ V (the open regime). (d) Hard gap spectroscopy of device C. $V_{\rm G2} = 0$ V. $V_{\rm G1}$ and $V_{\rm G2}$ are the voltages on the two tunnel gates. (e) A line cut from (d) at $V_{\rm G1} = -11.5$ V. (f) G vs V and $V_{\rm G2}$ in the more opened regime. $V_{\rm G1} = -4.8$ V. (g) Horizontal line cuts from (f) at $V = 0$ mV (blue) and -2.7 mV (red), respectively.

Device C is an island device[62] but operated as a tunneling spectroscopy device by setting one barrier region to be open (conductance much larger than $2e^2/h$). A hard gap with sharp coherence peaks can be observed in Figs. 4(d) and 4(e). The gap size is $\sim$1.3 meV. For all devices (A, B, C, and D), Fabry–Pérot-like oscillations

outside the gap are present. The oscillations for subgap conductance becomes noticeable in a more opened regime as shown in Figs. 4(f)–4(g) for device C. The quasiperiodic oscillations suggest two well-defined scattering points, likely the two barrier regions of the island device. Note that even if one barrier is tuned to be considerably open, it can still act as a scattering point in Fabry–Pérot oscillations.

In summary, we have observed a hard superconducting gap with sharp coherence peaks in PbTe nanowires coupled to a superconductor Pb. The gap size is ~ 1 meV, several times larger than that of Al. Our result may enable the search for high quality Majorana signatures in PbTe nanowires, as well as other PbTe-based hybrid superconducting quantum devices.

Acknowledgment. This work was supported by Tsinghua University Initiative Scientific Research Program, the National Natural Science Foundation of China (Grant No. 92065206), and the Innovation Program for Quantum Science and Technology (Grant No. 2021ZD0302400). S. Y. also acknowledges the support from National Postdoctoral Researcher Program of China (Grant No. GZC20231368). Raw data and processing codes within this paper are available at https://doi.org/10.5281/zenodo.8313595.

References

[1] Takei S, Fregoso B M, Hui H Y, Lobos A M, and Sarma S D 2013 *Phys. Rev. Lett.* **110** 186803
[2] Doh Y J, van Dam J A, Roest A L, Bakkers E P A M, Kouwenhoven L P, and Franceschi S D 2015 *Science* **309** 272
[3] Mourik V, Zuo K, Frolov S M, Plissard S, Bakkers E P, and Kouwenhoven L P 2012 *Science* **336** 1003
[4] Gül Ö, Zhang H, de Vries F K *et al.* 2017 *Nano Lett.* **17** 2690
[5] Zhang H, Gül Ö, Conesa-Boj S, Nowak M P *et al.* 2017 *Nat. Commun.* **8** 16025
[6] Chang W, Albrecht S, Jespersen T, Kuemmeth F, Krogstrup P, Nygård J, and Marcus C M 2015 *Nat. Nanotechnol.* **10** 232
[7] Krogstrup P, Ziino N, Chang W, Albrecht S, Madsen M, Johnson E, Nygård J, Marcus C, and Jespersen T 2015 *Nat. Mater.* **14** 400
[8] Zellekens P, Deacon R, Perla P *et al.* 2020 *Phys. Rev. Appl.* **14** 054019
[9] Pan D, Song H, Zhang S, Liu L, Wen L, Liao D, Zhuo R, Wang Z, Zhang Z, Yang S, Ying J, Miao W, Shang R, Zhang H, and Zhao J 2022 *Chin. Phys. Lett.* **39** 058101
[10] Deng M, Vaitiekėnas S, Hansen E B, Danon J, Leijnse M, Flensberg K, Nygård J, Krogstrup P, and Marcus C M 2016 *Science* **354** 1557
[11] Gül Ö, Zhang H, Bommer J D *et al.* 2018 *Nat. Nanotechnol.* **13** 192
[12] Song H, Zhang Z, Pan D, Liu D, Wang Z, Cao Z, Liu L, Wen L, Liao D, Zhuo R, Liu D E, Shang R, Zhao J, and Zhang H 2022 *Phys. Rev. Res.* **4** 033235
[13] Wang Z, Song H, Pan D, Zhang Z, Miao W, Li R, Cao Z, Zhang G, Liu L, Wen L, Zhuo R, Liu D E, He K, Shang R, Zhao J, and Zhang H 2022 *Phys. Rev. Lett.* **129** 167702
[14] Dvir T, Wang G, van Loo N, Liu C X, Mazur G, Bordin A, Haaf S, Wang J Y, Driel D, Zatelli F *et al.* 2023 *Nature* **614** 445
[15] Aghaee M, Akkala A, Alam Z *et al.* 2023 *Phys. Rev. B* **107** 245423
[16] Zhang H, Liu D E, Wimmer M, and Kouwenhoven L P 2019 *Nat. Commun.* **10** 5128
[17] Prada E, San-Jose P, de Moor M W, Geresdi A, Lee E J, Klinovaja J, Loss D, Nygård J, Aguado R, and Kouwenhoven L P 2020 *Nat. Rev. Phys.* **2** 575
[18] Cao Z, Chen S, Zhang G, and Liu D E 2023 *Sci. China Phys. Mech. Astron.* **66** 267003
[19] Larsen T W, Petersson K D, Kuemmeth F, Jespersen T S, Krogstrup P, Nygård J, and Marcus C M 2015 *Phys. Rev. Lett.* **115** 127001
[20] de Lange G, van Heck B, Bruno A, van Woerkom D J, Geresdi A, Plissard S R, Bakkers E P A M, Akhmerov A R, and DiCarlo L 2015 *Phys. Rev. Lett.* **115** 127002
[21] Tosi L, Metzger C, Goffman M F, Urbina C, Pothier H, Park S, Yeyati A L, Nygård J, and Krogstrup P 2019 *Phys. Rev. X* **9** 011010
[22] Hays M, Fatemi V, Bouman D, Cerrillo J, Diamond S, Serniak K, Connolly T, Krogstrup P, Nygård J, Yeyati A L, Geresdi A, and Devoret M H 2021 *Science* **373** 430
[23] Huo J, Xia Z, Li Z, Zhang S, Wang Y, Pan D, Liu Q, Liu Y, Wang Z, Gao Y, Zhao J, Li T, Ying J, Shang R, and Zhang H 2023 *Chin. Phys. Lett.* **40** 047302
[24] Pita-Vidal M, Bargerbos A, Žitko R *et al.* 2023 *Nat. Phys.* **19** 1110
[25] Lutchyn R M, Sau J D, and Das Sarma S 2010 *Phys. Rev. Lett.* **105** 077001
[26] Oreg Y, Refael G, and von Oppen F 2010 *Phys. Rev. Lett.* **105** 177002
[27] Liu J, Potter A C, Law K T, and Lee P A 2012 *Phys. Rev. Lett.* **109** 267002
[28] Rainis D, Trifunovic L, Klinovaja J, and Loss D 2013 *Phys. Rev. B* **87** 024515
[29] Pan H and Das Sarma S 2020 *Phys. Rev. Res.* **2** 013377
[30] Das Sarma S and Pan H 2021 *Phys. Rev. B* **103** 195158
[31] Zeng C, Sharma G, Tewari S, and Stanescu T 2022 *Phys. Rev. B* **105** 205122
[32] Cao Z, Liu D E, He W X, Liu X, He K, and Zhang H 2022 *Phys. Rev. B* **105** 085424
[33] Jiang Y, Yang S, Li L, Song W, Miao W, Tong B, Geng Z, Gao Y, Li R, Chen F, Zhang Q, Meng F, Gu L, Zhu K, Zang Y, Shang R, Cao Z, Feng X, Xue Q K, Liu D E, Zhang H, and He K 2022 *Phys. Rev. Mater.* **6** 034205
[34] Jung J, Schellingerhout S G, Ritter M F, ten Kate S C, van der Molen O A, de Loijer S, Verheijen M A, Riel H, Nichele F, and Bakkers E P 2022 *Adv. Funct. Mater.* **32** 2208974
[35] Geng Z, Zhang Z, Chen F, Yang S, Jiang Y, Gao Y, Tong B, Song W, Miao W, Li R, Wang Y, Zhang Q, Meng F, Gu L, Zhu K, Zang Y, Li L, Shang R, Feng X, Xue Q K, He K, and Zhang H 2022 *Phys. Rev. B* **105** L241112
[36] ten Kate S C, Ritter M F, Fuhrer A, Jung J, Schellingerhout S G, Bakkers E P A M, Riel H, and Nichele F 2022 *Nano Lett.* **22** 7049
[37] Song W, Wang Y, Miao W, Yu Z, Gao Y, Li R, Yang S, Chen F, Geng Z, Zhang Z, Zhang S, Zang Y, Cao Z, Liu D E, Shang R, Feng X, Li L, Xue Q K, He K, and Zhang H 2023 *Phys. Rev. B* **108** 045426
[38] Zhang Z, Song W, Gao Y, Wang Y, Yu Z, Yang S, Jiang Y, Miao W, Li R, Chen F, Geng Z, Zhang Q, Meng F, Lin T, Gu L, Zhu K, Zang Y, Li L, Shang R, Feng X, Xue Q K, He K, and Zhang H 2023 *Phys. Rev. Mater.* **7** 086201
[39] Kanne T, Marnauza M, Olsteins D, Carrad D, Sestoft J E, Bruijckere J, Zeng L, Johnson E, Olsson E, Grove-Rasmussen K, and Nygård J 2021 *Nat. Nanotechnol.* **16** 776
[40] Dynes R C, Narayanamurti V, and Garno J P 1978 *Phys. Rev. Lett.* **41** 1509
[41] Pillet J, Quay C, Morfin P, Bena C, Yeyati A L, and Joyez P 2010 *Nat. Phys.* **6** 965

[42] Dirks T, Hughes T L, Lal S, Uchoa B, Chen Y F, Chialvo C, Goldbart P M, and Mason N 2010 *Nat. Phys.* **7** 386
[43] Lee E J, Jiang X, Houzet M, Aguado R, Lieber C M, and De Franceschi S 2014 *Nat. Nanotechnol.* **9** 79
[44] Zhang S, Wang Z, Pan D, Li H, Lu S, Li Z, Zhang G, Liu D, Cao Z, Liu L, Wen L, Liao D, Zhuo R, Shang R, Liu D E, Zhao J, and Zhang H 2022 *Phys. Rev. Lett.* **128** 076803
[45] Wang Z, Zhang S, Pan D, Zhang G, Xia Z, Li Z, Liu D, Cao Z, Liu L, Wen L, Liao D, Zhuo R, Li Y, Liu D E, Shang R, Zhao J, and Zhang H 2022 *Phys. Rev. B* **106** 205421
[46] Prada E, San-Jose P, and Aguado R 2012 *Phys. Rev. B* **86** 180503
[47] Kells G, Meidan D, and Brouwer P 2012 *Phys. Rev. B* **86** 100503
[48] Liu C X, Sau J D, Stanescu T D, and Sarma S D 2017 *Phys. Rev. B* **96** 075161
[49] Reeg C, Dmytruk O, Chevallier D, Loss D, and Klinovaja J 2018 *Phys. Rev. B* **98** 245407
[50] Moore C, Zeng C, Stanescu T D, and Tewari S 2018 *Phys. Rev. B* **98** 155314
[51] Vuik A, Nijholt B, Akhmerov A, and Wimmer M 2019 *SciPost Phys.* **7** 061
[52] Cao Z, Zhang H, Lü H F, He W X, Lu H Z, and Xie X C 2019 *Phys. Rev. Lett.* **122** 147701
[53] Wang Y, Chen F, Song W, Geng Z, Yu Z, Yang L, Gao Y, Li R, Yang S, Miao W, Xu W, Wang Z, Xia Z, Song H D, Feng X, Wang T, Zang Y, Li L, Shang R, Xue Q, He K, and Zhang H 2023 *Nano Lett.* **23** 11137
[54] Blonder G, Tinkham M M, and Klapwijk K T 1982 *Phys. Rev. B* **25** 4515
[55] Beenakker C W J 1992 *Phys. Rev. B* **46** 12841
[56] Liu C X, Setiawan F, Sau J D, and Das Sarma S 2017 *Phys. Rev. B* **96** 054520
[57] Bommer J D, Zhang H, Gül Ö *et al.* 2019 *Phys. Rev. Lett.* **122** 187702
[58] Grove-Rasmussen K, Jørgensen H I, Andersen B M, Paaske J, Jespersen T S, Nygård J, Flensberg K, and Lindelof P E 2009 *Phys. Rev. B* **79** 134518
[59] Andersen B M, Flensberg K, Koerting V, and Paaske J 2011 *Phys. Rev. Lett.* **107** 256802
[60] Lee E J H, Jiang X, Aguado R, Katsaros G, Lieber C M, and De Franceschi S 2012 *Phys. Rev. Lett.* **109** 186802
[61] He J, Pan D, Yang G, Liu M, Ying J, Lyu Z, Fan J, Jing X, Liu G, Lu B, Liu D E, Zhao J, Lu L, and Qu F 2020 *Phys. Rev. B* **102** 075121
[62] Albrecht S, Higginbotham A, Madsen M, Kuemmeth F, Jespersen T, Nygård J, Krogstrup P, and Marcus C 2016 *Nature* **531** 206